Decoherence, matter effect, and neutrino hierarchy signature in long baseline experiments

João A. B. Coelho and W. Anthony Mann

Phys. Rev. D **96**, 093009 — Published 27 November 2017

DOI: 10.1103/PhysRevD.96.093009

Decoherence, matter effect, ν hierarchy signature in long-baseline experiments

João A. B. Coelho[1, 2, *] and W. Anthony Mann[1, †]

[1] *Physics Department, Tufts University, Medford, Massachusetts 02155, USA*
[2] *APC, Université Paris Diderot, CNRS/IN2P3, Sorbonne Paris Cité, F-75205 Paris, France*

Environmental decoherence of oscillating neutrinos of strength $\Gamma = (2.3 \pm 1.1) \times 10^{-23}$ GeV can explain how maximal θ_{23} mixing observed at 295 km by T2K appears to be non-maximal at longer baselines. As shown recently by R. Oliveira, the MSW matter effect for neutrinos is altered by decoherence: In normal (inverted) mass hierarchy, a resonant enhancement of $\nu_\mu(\bar{\nu}_\mu) \to \nu_e(\bar{\nu}_e)$ occurs for $6 < E_\nu < 20$ GeV. Thus decoherence at the rated strength may be detectable as an excess of charged-current ν_e events in the full ν_μ exposures of MINOS+ and OPERA.

PACS numbers: 14.60.Pq, 14.60.St, 13.15.+g

I. INTRODUCTION

A. ν decoherence in long-baseline experiments

Neutrino flavor oscillations are the consequence of quantum mechanical mixing between mass and flavor eigenstates. The mixing is generally regarded to be fully described by the PMNS matrix which is conventionally parameterized using three mixing angles, θ_{12}, θ_{13}, θ_{23}, and a CP violating phase, δ_{CP} [1]. For nearly two decades neutrino oscillation experiments have indicated the θ_{23} angle, which characterizes flavor mixing of the 'atmospheric' $\mu - \tau$ flavor sector, is compatible with the maximal value of 45^o (i.e. $\sin^2\theta_{23} = 0.5$). A close-to-maximal value for θ_{23} is very intriguing because it implies that the ν_3 mass eigenstate is comprised of ν_μ and ν_τ flavors in nearly equal amounts. Recently however, there is an indication from the NOvA long-baseline neutrino oscillation experiment that in ν_μ disappearance oscillations observed at 810 km, flavor mixing in the atmospheric sector deviates from maximal mixing. This indication for non-maximal mixing in NOvA data is reported to be at the level of $2.6\,\sigma$ [2]. In a recent global analysis maximal mixing is disfavored at the $2\,\sigma$ level [3]. The NOvA result is in tension with the 295-km baseline measurements of T2K [4], and it undermines the idea that the PMNS lepton-flavor mixing matrix harbors an exact $\mu-\tau$ flavor symmetry [5]. In a recent paper the authors proposed that neutrino decoherence that is environmentally-induced can help to alleviate this tension. It is proposed that θ_{23} may in fact be nearly maximal and that the apparent tension can be lifted by neutrino decoherence of coupling strength, Γ, in a specified range whose influence becomes more pronounced with increasing oscillation baselines [6]. Previous studies of neutrino decoherence have considered various integer power-law forms for the decoherence parameter: $\Gamma = \Gamma_0 \cdot (\frac{E_\nu}{[GeV]})^n$ [7–9]. For experiments that have similar ratios of baseline to neutrino energy, L/E_ν, such as T2K and NOvA however, the tension cannot be alleviated by a negative-integer power-law model. On the other hand, decoherence effects that ensue with a positive-integer power law form are constrained by atmospheric neutrino data [7]. The model considered by this work assumes decoherence to be characterized by a coupling parameter that is energy-independent and of strength $\Gamma = (2.3 \pm 1.1) \times 10^{-23}$ GeV [6]. Decoherence of this form introduces a small, exponential damping of neutrino oscillations that mimics the effect of non-maximal θ_{23} mixing when interpreted by conventional 3-flavor neutrino-oscillation analyses.

Decoherence is observed in a variety of quantum systems that are "open" to environmental influences, and the phenomenology for describing decoherence effects in these systems is well developed [10]. For evolving neutrino states, the pervasive environment might originate in couplings to new physics beyond the standard electroweak model, e.g. perturbations arising from spacetime itself and its Planck-scale dynamics [7, 11, 12].

To be clear, environmentally induced decoherence is to be distinguished from neutrino wave-packet decoherence, a quantum wave effect that one may expect to occur based on known physics [13, 14]. While wave-packet decoherence also introduces exponential damping factors that multiply the oscillatory terms in the oscillation transition probabilities, the damping depends strongly on the neutrino energy as well as on the baseline. Consequently wave-packet decoherence is not viable as an effect that can account for the emergence of apparent nonmaximal neutrino mixing with a longer baseline [6].

The purpose of this paper is to highlight a remarkable prediction concerning neutrino decoherence and to show, with numerical analyses, that experimental detection of a specific decoherence signature is currently within the reach of the MINOS+ and OPERA accelerator-based long-baseline experiments.

B. ν decoherence alters the matter effect

Neutrino environmental decoherence, if present, may conspire with the terrestrial MSW matter effect [15] to give a small resonant peak in ν_e-flavor appearance oscilla-

* jcoelho@apc.in2p3.fr
† anthony.mann@tufts.edu

tions in the neutrino energy range $6 < E_\nu < 20$ GeV. As will be elaborated in this work, an enhancement in the charged current (CC) ν_e-flavor rate is predicted which is large enough to be observable by current-generation accelerator-based long-baseline experiments. That is, neutrino decoherence would enable the MSW matter effect to provide the same hierarchy signature that, sans decoherence, could only appear with baselines that predominantly involve mantle traversal. Observation of this enhancement in $\nu_\mu(\bar{\nu}_\mu) \to \nu_e(\bar{\nu}_e)$ oscillations would, at once, be strong evidence for neutrino environmental decoherence and for the normal (inverted) mass hierarchy.

The unusual interplay between neutrino decoherence and the MSW matter effect was first uncovered by Roberto Oliveira, who considered its implications for oscillation measurements at DUNE [16]. Unfortunately, as Oliveira acknowledged, the resonant enhancement is likely beyond the reach of the neutrino beams envisaged for DUNE, whose flux spectral peaks are in the range 2.5 to ~ 3.0 GeV [17] and whose intensities by $E_\nu \sim 8$ GeV are down by 1.5 orders-of-magnitude. The situation is even less favorable with the off-axis NuMI beam to NOvA; the beam, by design, is narrow-band with the spectral peak located at 2 GeV. With the medium-energy exposure of MINOS+ to the on-axis NuMI beam at Fermilab however, the possibility exists for detection of this decoherence - matter effect "conspiracy".

C. Overview

We begin with a heuristic derivation of $\nu_\mu \to \nu_e$ appearance oscillations with inclusion of decoherence. We use minimalist phenomenology to show how decoherence enters into the familiar leading-order oscillation formulas for 3-flavor oscillations with matter effects and how it modifies the relationship between the oscillation amplitude and the oscillation phase. We arrive at the same decoherence parametrization presented in our previous work and its forms, albeit approximate, exhibit the essential physics. More accurate, albeit complicated, analytic forms are available in the literature [16], and more considered justifications concerning the reduction of coupling parameters can be found in [6] and elsewhere [16, 18–22].

Precise numerical methods are then used to calculate the probabilities for the $\nu_\mu(\bar{\nu}_\mu) \to \nu_e(\bar{\nu}_e)$ transition in current long-baseline experiments. The latter calculations represent a full three-flavor plus matter effects treatment, taking into account the solar-scale mixing and CP-violation contributions that are neglected in our heuristic analytic result. With the oscillation-with-decoherence probabilities in hand, we consider the prospects for detection of the decoherence-driven enhancement in $\nu_\mu(\bar{\nu}_\mu) \to \nu_e(\bar{\nu}_e)$ predicted to occur in the vicinity of the terrestrial MSW resonance at $E_\nu \sim 12$ GeV $\left(\frac{\Delta m^2_{31}}{2.52\times10^{-3}\ \mathrm{eV}^2}\right)\left(\frac{2.75\ \mathrm{g/cm}^3}{\rho}\right)$. OPERA and MINOS+ are experiments whose beams give non-negligible event rates in their far detectors in the energy region $6 < E_\nu < 20$ GeV. Preliminary results from the OPERA experiment's search for ν_e appearance do not show an excess of events, however the event statistics are low in the relevant region of E_ν. The MINOS+ experiment will isolate a candidate sample with higher statistics but with much larger backgrounds, assuming that the experiment analyzes its full medium-energy exposure of 10^{21} POT into ν_μ neutrinos of the NuMI beam at Fermilab. The search by MINOS+ can be augmented by examining events recorded by the earlier MINOS exposures in the low-energy NuMI beam.

The neutrino fluxes and/or flux-times-cross-section event rates per exposure protons-on-target (POT) have been reported by MINOS, MINOS+, and OPERA at conferences, as have their event rates after selection for multi-GeV CC ν_e-like events. Based on this information we have assembled rough predictions for the ν_e rate excess that these experiments should see if indeed decoherence is operative and neutrino masses follow the normal mass hierarchy. We find that the preliminary data analyses presented by OPERA and MINOS+ point towards opposite conclusions. We conclude by urging for more focussed experimental effort to shed light on the remarkable possibility that environmental decoherence engages with the MSW matter effect to open a window onto the ordering of neutrino masses.

II. DECOHERENCE UNLOCKS MATTER EFFECT IN $\nu_\mu \to \nu_e$ OSCILLATION

That environmental decoherence may conspire to save the MSW matter effect from self-imposed irrelevance in current long-baseline oscillation experiments is an important result that is generally not appreciated. The mechanism by which this happens, however, can be readily elicited by considering analytic forms for the $\nu_\mu \to \nu_e$ transition in matter in the presence of decoherence.

For neutrino states considered as a closed system, time evolution is governed by the total Hamiltonian $\hat{H} = \hat{H}_{osc} + \hat{V}_{matter}$. Since $\hat{H}$ is hermitian, there is a basis spanned by neutrino effective mass states wherein $\hat{H}$ is diagonal:

$$\hat{H} = \mathrm{diag}\,(\tilde{E}_1, \tilde{E}_2, \tilde{E}_3)_{\tilde{m}} \tag{1}$$

For the elements we write $\tilde{E}_i \equiv \tilde{m}_i^2/2E_\nu$, associating energy levels to effective neutrino masses in analogy to oscillations described in vacuum. The importance of differences in the squared effective masses can be seen upon re-phasing the Hamiltonian, an algebraic manipulation leading to removal of a term proportional to $\hat{\mathbb{I}}$ which merely contributes an overall phase to the oscillation amplitudes. The re-phased Hamiltonian is

$$\hat{H} = \frac{1}{2E_\nu}\mathrm{diag}(0, \Delta\tilde{m}^2_{21}, \Delta\tilde{m}^2_{31})_{\tilde{m}}. \tag{2}$$

From low energy measurements, where matter effects are negligible, the neutrino masses are known to follow the pattern $|m_2^2 - m_1^2| \ll |m_3^2 - m_1^2|$, i.e. $|\Delta m^2_{31}| \simeq |\Delta m^2_{32}| \gg |\Delta m^2_{21}|$. Furthermore, for the baselines, L, and neutrino energies, E_ν that characterize the accelerator-based long-baseline experiments, $\Delta m^2_{21} L/4E_\nu \ll 1$. The contribution from Δm^2_{21} in vacuum may thus be neglected. Additionally we neglect the Dirac CP phase, $\delta_{CP} \to 0$. (Below we show complex conjugations of mixing matrix elements, even though they have no effect in our formulas.)

For accelerator neutrinos evolving/propagating sans decoherence, time in natural units equals the propagation distance, L, and the oscillatory phase is conveniently expressed as $\Delta \cdot L$ using the form $\Delta \equiv (\Delta m^2_{31}/4E_\nu)$. Under these assumptions, the re-phased Hamiltonian can be easily solved analytically yielding

$$\hat{H} \simeq 2\Delta \, \mathrm{diag}(0, \tilde{\xi}_-, \tilde{\xi}_+)_{\tilde{m}}, \tag{3}$$

where the matter-effective phases that describe neutrino oscillations in matter of constant density [27, 28] are

$$\begin{aligned} \tilde{\xi}_\pm &= \frac{1}{2}\left[\hat{A} + 1 \pm \tilde{\xi}_0\right], \quad \text{and} \\ \tilde{\xi}_0 &= \sqrt{\sin^2 2\theta_{13} + (\cos 2\theta_{13} - \hat{A})^2}. \end{aligned} \tag{4}$$

Here, $\hat{A}$ is the terrestrial matter potential,

$$\hat{A} = \pm \frac{\sqrt{2}\, G_F \, n_e}{2\Delta} \tag{5}$$

where G_F is the Fermi constant, n_e is the electron density in matter, and the $+$ $(-)$ sign applies to neutrinos (antineutrinos). From equations (2) and (3), we can then derive the following associations:

$$\begin{aligned} \tilde{\Delta}_{21} &\approx \Delta \, \tilde{\xi}_-, \\ \tilde{\Delta}_{31} &\approx \Delta \, \tilde{\xi}_+, \\ \tilde{\Delta}_{32} &\approx \Delta \, \tilde{\xi}_0. \end{aligned} \tag{6}$$

In the absence of decoherence, the time evolution of neutrino states is governed by the effective Schrödinger wave equation or equivalently, using density matrices for pure states, by the von Neumann equation.

With environmental decoherence operative however, the neutrino states no longer comprise an isolated system. Their coupling to the environment has consequences for time evolution which are embodied by the Lindblad master equation. The presence of weakly perturbative dynamics is parameterized by a "dissipator" term, $\mathcal{D}[\hat{\rho}(t)]$, added to the von Neumann equation [23, 24]. We undertake to solve the Lindblad equation, starting with the Hamiltonian of Eq. (1) and the density matrix $\rho_{\tilde{m}}(t)$ expressed in the effective mass basis:

$$\frac{d}{dt}\hat{\rho}_{\tilde{m}}(t) = -i[\hat{H}, \hat{\rho}_{\tilde{m}}(t)] - \mathcal{D}[\hat{\rho}_{\tilde{m}}(t)]. \tag{7}$$

The general form of the dissipator is determined by the requirement of *complete positivity* [24, 25]. It is constructed using a set of $N^2 - 1$ operators, $\hat{D}_n$, where N is the dimension of the Hilbert space of interest. So, for three-flavor neutrino oscillations $N = 3$ and the $\hat{D}_n$ can, for example, be expressed as linear combinations of the Gell-Mann matrices.

$$\begin{aligned} &\mathcal{D}[\hat{\rho}_{\tilde{m}}(t)] = \\ &\sum_{n=1}^{8} \left(\{\hat{\rho}_{\tilde{m}}(t), \hat{D}_n^\dagger \hat{D}_n\}_+ - 2\hat{D}_n \hat{\rho}_{\tilde{m}}(t) \hat{D}_n^\dagger \right). \end{aligned} \tag{8}$$

Constraints are imposed on the $\hat{D}_n$ arising from mathematical considerations and from the laws of thermodynamics. Specifically, it is assumed that the von Neumann entropy, $S = -Tr(\hat{\rho}\ln\hat{\rho})$, increases with time and this is enforced by requiring the $\hat{D}_n$ to be hermitian. In addition, conservation of the average energy of the system, calculated as $Tr(\hat{\rho}\,\hat{H})$, is assured by requiring $[\hat{D}_n, \hat{H}] = 0$ for all $\hat{D}_n$. Thus average conservation of energy implies that the $\hat{D}_n$ and $\hat{H}$ can be simultaneously diagonalized.

Our approach to a solution follows the phenomenological approach presented in Ref. [26], however here we assume that the basis in which the simultaneous diagonalization happens, i.e. the basis in which the conservation of energy is defined, is not the neutrino mass basis, but rather the effective mass basis:

$$\hat{D}_n = \mathrm{diag}\,(d_{n,1}, d_{n,2}, d_{n,3})_{\tilde{m}}. \tag{9}$$

Considering the nth term in the dissipator as indicated by the right-hand side of Eq. (8), the anticommutator of $\hat{\rho}_{\tilde{m}}(t)$ with the product $\hat{D}_n^\dagger \hat{D}_n = \mathrm{diag}\,(d^2_{n,1}, d^2_{n,2}, d^2_{n,3})$ gives

$$\begin{aligned} &\{\hat{\rho}_{\tilde{m}}(t), \hat{D}_n^\dagger \hat{D}_n\}_+ = \\ &\begin{pmatrix} 2d^2_{n,1}\,\rho_{11} & (d^2_{n,1} + d^2_{n,2})\,\rho_{12} & (d^2_{n,1} + d^2_{n,3})\,\rho_{13} \\ (d^2_{n,1} + d^2_{n,2})\,\rho_{21} & 2d^2_{n,2}\,\rho_{22} & (d^2_{n,2} + d^2_{n,3})\,\rho_{23} \\ (d^2_{n,1} + d^2_{n,3})\,\rho_{31} & (d^2_{n,2} + d^2_{n,3})\,\rho_{32} & 2d^2_{n,3}\,\rho_{33} \end{pmatrix} \end{aligned} \tag{10}$$

Upon addition of the second part of the nth term, $-2\hat{D}_n\,\hat{\rho}_{\tilde{m}}(t)\,\hat{D}_n^\dagger$, with the anticommutator, the diagonal elements of (10) are canceled and the off-diagonal elements become amenable to completion-of-squares. Summing over all eight terms gives constant, positive-valued decoherence couplings in the off-diagonal elements that we write as

$$\Gamma_{ij} = \Gamma_{ji} = \sum_{n=1,8} (d_{n,i} - d_{n,j})^2. \tag{11}$$

Thus the dissipator term in effective mass basis is

$$-\mathcal{D}[\hat{\rho}_{\tilde{m}}(t)] = \begin{pmatrix} 0 & -\Gamma_{21}\,\rho_{12}(t) & -\Gamma_{31}\,\rho_{13}(t) \\ -\Gamma_{21}\,\rho_{21}(t) & 0 & -\Gamma_{32}\,\rho_{23}(t) \\ -\Gamma_{31}\,\rho_{31}(t) & -\Gamma_{32}\,\rho_{32}(t) & 0 \end{pmatrix}. \tag{12}$$

Adding matrix (12) to the von Neumann commutator in the right-hand side of Eq. (7) gives the Lindblad equation in matrix form. First integration of each element yields

$$\hat{\rho}_{\tilde{m}}(t) = \begin{pmatrix} \rho_{11}(0) & \rho_{12}(0)\,e^{-\eta_{21}^* t} & \rho_{13}(0)\,e^{-\eta_{31}^* t} \\ \rho_{21}(0)\,e^{-\eta_{21} t} & \rho_{22}(0) & \rho_{23}(0)e^{-\eta_{32}^* t} \\ \rho_{31}(0)e^{-\eta_{31} t} & \rho_{32}(0)e^{-\eta_{32} t} & \rho_{33}(0) \end{pmatrix}. \tag{13}$$

where we have introduced the notation $\eta_{ij} \equiv (\Gamma_{ij} + i2\tilde{\Delta}_{ij})$.

For our purposes it suffices to assume that only a single $\hat{D}_n$ operator is active: $\hat{D}_n = \mathrm{diag}(d_1, d_2, d_3)$. Its eigenvalues are real, positive-valued, quantities with dimension of energy, which we assume to be related in a way that mimics the neutrino mass pattern $|m_2^2 - m_1^2| \ll |m_3^2 - m_1^2|$, namely $(d_2 - d_1)^2 \ll (d_3 - d_1)^2$. Additionally, in order to focus on the dominant decoherence effect, we assume that $(d_2 - d_1)^2 \simeq 0$ and can be ignored. The latter assumption together with Eq. (11) reduces the set of decoherence couplings to a single parameter, Γ:

$$\Gamma_{21} = 0 \;\; \text{and} \;\; \Gamma \equiv \Gamma_{31} = \Gamma_{32}. \tag{14}$$

The initial neutrino state $|\nu_\mu\rangle$ is represented in the effective mass basis by the density matrix $\rho_{\tilde{m}}^{(\mu)}(0)$ whose elements are

$$\hat{\rho}_{\tilde{m}}^{(\mu)}(0) = \tilde{U}^T \cdot \hat{\Pi}^{\nu_\mu} \cdot \tilde{U}^* \;\; \Leftrightarrow \;\; \left[\rho_{\tilde{m}}^{(\mu)}(0)\right]_{ij} = \tilde{U}_{\mu i}\tilde{U}_{\mu j}^*. \tag{15}$$

Here we refer to the state projector in neutrino flavor basis $\hat{\Pi}^{\nu_\mu} \equiv |\nu_\mu\rangle\langle\nu_\mu| \equiv \mathrm{diag}(0,1,0)_\alpha$, and to the PMNS mixing matrix with matter-effective elements:

$$\tilde{U} = \begin{pmatrix} \tilde{U}_{e1} & \tilde{U}_{e2} & \tilde{U}_{e3} \\ \tilde{U}_{\mu 1} & \tilde{U}_{\mu 2} & \tilde{U}_{\mu 3} \\ \tilde{U}_{\tau 1} & \tilde{U}_{\tau 2} & \tilde{U}_{\tau 3} \end{pmatrix}. \tag{16}$$

The unusual-looking form of the unitary transformation indicated in Eq. (15) reflects the convention $|\nu(0)\rangle = |\nu_\alpha\rangle = U_{\alpha j}^* |\nu_j\rangle$.

Insertion of the initial-state elements of Eq. (15) into Eq. (13) yields the time-evolved density matrix:

$$\hat{\rho}_{\tilde{m}}{}^{(\mu)}(t = L) = \begin{pmatrix} |\tilde{U}_{\mu 1}|^2 & \tilde{U}_{\mu 1}\tilde{U}_{\mu 2}^*\,e^{-\eta_{21}^* L} & \tilde{U}_{\mu 1}\tilde{U}_{\mu 3}^*\,e^{-\eta_{31}^* L} \\ \tilde{U}_{\mu 2}\tilde{U}_{\mu 1}^*\,e^{-\eta_{21} L} & |\tilde{U}_{\mu 2}|^2 & \tilde{U}_{\mu 2}\tilde{U}_{\mu 3}^*\,e^{-\eta_{32}^* L} \\ \tilde{U}_{\mu 3}\tilde{U}_{\mu 1}^*\,e^{-\eta_{31} L} & \tilde{U}_{\mu 3}\tilde{U}_{\mu 2}^*\,e^{-\eta_{32} L} & |\tilde{U}_{\mu 3}|^2 \end{pmatrix}. \tag{17}$$

To obtain the ν_e appearance probability at baseline L, we transform the density matrix into the neutrino flavor basis $\{|\nu_\alpha\rangle, \alpha = e, \mu, \tau\}$:

$$\rho_\alpha^{(\mu)}(t) = \tilde{U}^* \cdot \rho_{\tilde{m}}^{(\mu)}(t) \cdot \tilde{U}^T. \tag{18}$$

The state projector for the final state in $\nu_\mu \to \nu_e$ appearance oscillations, $|\nu_e\rangle$, is $\hat{\Pi}^{\nu_e} \equiv |\nu_e\rangle\langle\nu_e| \equiv \mathrm{diag}(1,0,0)_\alpha$, and the ν_e appearance probability is calculated as

$$\mathcal{P}_{(\nu_\mu \to \nu_e)} = Tr\left[\hat{\Pi}^{\nu_e} \cdot \rho_\alpha^{(\mu)}(t)\right] = \langle\nu_e|\,\rho_\alpha^{(\mu)}(t)\,|\nu_e\rangle, \tag{19}$$

or equivalently,

$$\mathcal{P}_{(\nu_\mu \to \nu_e)} = \sum_{i,j} \tilde{U}_{ei}^* \tilde{U}_{ej} \left[\rho_{\tilde{m}}^{(\mu)}(t)\right]_{ij}. \tag{20}$$

Due to the symmetry introduced by neglecting the solar scale mass-square splitting, it can be shown that, for neutrinos (antineutrinos), the effective solar mixing angle $\tilde{\theta}_{12} = \pi/2$ (0), i.e. $\tilde{U}_{e1} = 0$ ($\tilde{U}_{e2} = 0$). Writing out Eq. (20) explicitly, and taking $U_{e1} = 0$, the appearance probability becomes

$$\begin{aligned} \mathcal{P}_{(\nu_\mu \to \nu_e)} &= |\tilde{U}_{e2}|^2|\tilde{U}_{\mu 2}|^2 + |\tilde{U}_{e3}|^2|\tilde{U}_{\mu 3}|^2 \\ &\quad + 2\,\mathcal{R}e\{\tilde{U}_{e2}^*\tilde{U}_{e3}\tilde{U}_{\mu 2}\tilde{U}_{\mu 3}^* e^{-(\Gamma - 2i\tilde{\Delta}_{32}L)}\}. \end{aligned} \tag{21}$$

To facilitate comparison with commonly used probability expressions, we re-express the mixing matrix amplitudes in terms of the matter-effective mixing angles. With neglect of solar-scale mixing, the mixing-matrix elements are given by

$$\begin{aligned} \tilde{U} &= U_{23}(\theta_{23})\,\tilde{U}_{13}(\tilde{\theta}_{13}, \delta_{CP} = 0)\,U_{12}(\theta_{12} = \pi/2) \\ &= U_{23}\,\tilde{U}_{13} = \begin{pmatrix} 0 & \tilde{c}_{13} & \tilde{s}_{13} \\ -c_{23} & -\tilde{s}_{13}s_{23} & \tilde{c}_{13}s_{23} \\ s_{23} & -\tilde{s}_{13}c_{23} & \tilde{c}_{13}c_{23} \end{pmatrix}. \end{aligned} \tag{22}$$

Evaluating the mixing amplitudes and using the identity $c_\theta s_\theta = s_{2\theta}/2$, we obtain

$$\mathcal{P}_{(\nu_\mu \to \nu_e)} = \sin^2 2\tilde{\theta}_{13} \cdot \sin^2\theta_{23} \cdot \frac{1}{2}[1 - e^{-\Gamma L}\cos(2\tilde{\Delta}_{32}L)]. \tag{23}$$

The matter-effective mixing angle $\tilde{\theta}_{13}$ is given by

$$\tan 2\tilde{\theta}_{13} \simeq \frac{\sin 2\theta_{13}}{\cos 2\theta_{13} - \hat{A}}. \tag{24}$$

The antineutrino probability can be written in exactly the same form, with the single replacement $\tilde{\Delta}_{32} \to \tilde{\Delta}_{31}$.

Equation (23) gives the leading-order transition probability for $\nu_\mu \to \nu_e$ oscillations in the presence of environmental decoherence. It is readily seen that in the limit $\Gamma \to 0$, the exponential damping factor becomes unity and allows the oscillatory $\cos(2\tilde{\Delta}_{32}L)$ term to combine with the first term via the identity $(1 - c_{2\phi}) = 2s_\phi^2$ to

give the well-known, conventional ν_e appearance probability [29, 30],

$$\mathcal{P}_{(\nu_\mu\to\nu_e)} = \sin^2(2\tilde{\theta}_{13})\cdot\sin^2\theta_{23}\cdot\sin^2(\tilde{\Delta}_{32}L). \qquad (25)$$

Comparing the conventional result (25) to oscillations with decoherence in-play, Eq. (23), one sees that the decoherence damping factor prevents the oscillation $\cos(2\tilde{\Delta}_{32}L)$ from being rolled together with the first term to give the conventional oscillatory behavior, $\sin^2(\tilde{\Delta}_{32}L)$. Referring to Eq. (23), the presence of damping permits oscillatory cosine term - in the vicinity of MSW - to swing sufficiently far below 1.0 to give an enhancement in ν_e appearance.

These points are readily illustrated with numerical considerations; we use the OPERA/MINOS baseline of ∼730 km as representative. The MSW resonance occurs in the vicinity of $E_\nu \sim 12$ GeV. At the resonance, $(\cos 2\theta_{13} - \hat{A}) \approx 0$, $\sin^2 2\tilde{\theta}_{13} \to 1$, and $\tilde{\Delta}_{32} \to \Delta\cdot\sin 2\theta_{13}$. Taking $\theta_{13} = 8.5^\circ$ as representative of the world-average value, we have $\sin 2\theta_{13} = \sin(17^\circ) \simeq 0.3$. Consequently the conventional oscillation phase at the value of E_ν that corresponds to the first oscillation maximum at 730 km, namely 1.5 GeV, gives $\sin^2(\frac{\pi}{2}\cdot\frac{1.5}{12}\cdot 0.3) \simeq \sin^2(\frac{\pi}{2}\cdot 0.04) \simeq 0.003$. Thus the oscillation phase shuts down the probability for ν_e appearance oscillations, even though the effective mixing angles are at maximal strength.

But with decoherence $\Gamma = 2.3\times10^{-23}$ GeV in play, the oscillation phase exerts influence in a different way. At the MSW resonance, Eq. (23) becomes

$$\mathcal{P}_{(\nu_\mu\to\nu_e)} \simeq 1\cdot\frac{1}{2}\cdot\frac{1}{2}\cdot[1 - e^{-\Gamma L}\cdot\cos(\pi\cdot 0.04)]. \qquad (26)$$

The cosine function is still close to 1.0 but is now damped by decoherence, consequently the MSW effect is still rendered to be small, but not zero: $\mathcal{P}_{(\nu_\mu\to\nu_e)} \simeq 0.022$.

III. NUMERICAL CALCULATIONS

The oscillation probabilities used in our analysis are derived from an exact formulation of Eq. (20), where the effective mixing elements of the PMNS matrix and the effective mass-square splittings were computed numerically through the diagonalization of the matter perturbed Hamiltonian. A full three flavor treatment was implemented and the following values of the neutrino oscillation parameters were used [31]: $\sin^2\theta_{12} = 0.306$, $\sin^2\theta_{13} = 0.02166$, $\delta_{CP} = 1.45\pi$, $\Delta m^2_{21} = 7.50\times10^{-5}\,\mathrm{eV}^2$, and $\Delta m^2_{31} = +2.524\times10^{-3}\,\mathrm{eV}^2$. In our decoherence scenario [6], the θ_{23} angle is assumed to be maximal, i.e. $\sin^2\theta_{23} = 0.5$. The density of matter is taken to be constant at a value of $\rho = 2.8\,\mathrm{g/cm}^3$.

Results from numerical calculation of probabilities for the $\nu_\mu \to \nu_e$ transition are shown in Fig. 1, for the baselines of T2K (295 km), MINOS+ (735 km), and DUNE (1300 km); the probabilities shown are for the normal mass hierarchy case. For each baseline, the probability for oscillation with decoherence (dashed curve) is displayed together with the expectation for conventional 3-flavor oscillation (solid curve). The comparisons thus provided show decoherence to diminish the transition in the main oscillation peak while promoting a secondary enhancement at higher E_ν in the vicinity of the MSW resonance. The strength of both trends is seen to grow as the observational baseline is extended. Probabilities for the OPERA (730 km) and NOvA (810 km) baselines are, of course, very nearly the same as those shown for MINOS+.

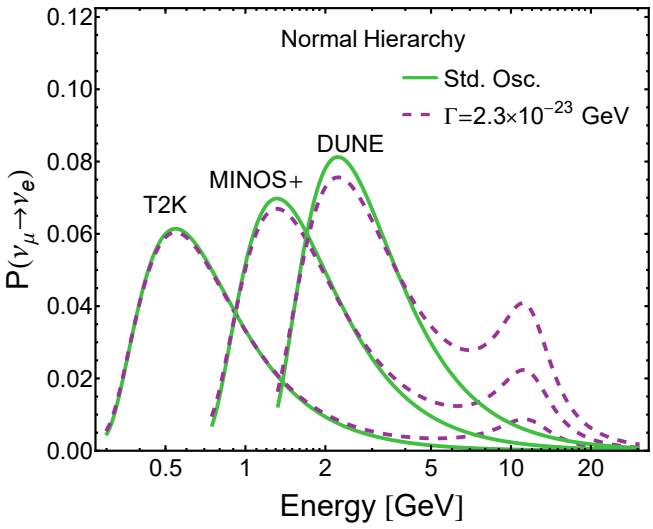

FIG. 1. Probability versus E_ν for $\nu_\mu \to \nu_e$ oscillations with environmental decoherence of strength Γ(dashed curve) for current long-baseline experiments, assuming the normal mass hierarchy. In the case that the effective energy basis is the eigenbasis for the environmental "measurement", decoherence conspires with the terrestrial MSW matter effect to give a small ν_e appearance maximum at 12 GeV.

IV. PROSPECTS FOR DETECTION

The current generation of accelerator-based, long-baseline neutrino oscillation experiments was optimized to measure the parameters that govern Standard-Model (SM) 3-flavor neutrino mixing using ν_μ-flavor disappearance and ν_e-flavor appearance measurements. Unfortunately those optimizations mitigate against beams with abundant fluxes in the vicinity of the terrestrial MSW matter effect at $E_\nu \sim 12$ GeV. For example, T2K is matched to a muon-neutrino beam whose flux spectrum peaks at 0.6 GeV and becomes negligible above 2-3 GeV. Similarly NOvA operates off-axis in the NuMI beam at Fermilab, an arrangement that provides a narrow-band flux peaked near 2 GeV. Prior to data-taking by NOvA, the MINOS experiment, whose far detector lies on-axis with respect to the NuMI beam, obtained all of its exposures with NuMI operated in its low-energy mode. This

configuration gave a wide-band spectrum with flux peak at $\sim 3\,\mathrm{GeV}$, and MINOS used it to obtain a total exposure of 10.56×10^{20} POT.

NOvA's off-axis low-energy beam is obtained by operating the NuMI beam line in its medium energy mode. In that mode the on-axis ν_μ beam is wide-band, with spectral peak at 7 GeV and with fluxes of useful intensity extending to ≥ 12 GeV. When the NuMI beam switched to extended medium-energy running for NOvA, MINOS became the MINOS+ experiment, which subsequently recorded a total exposure of 10×10^{20} POT in the on-axis, medium-energy NuMI beam. It is the addition of this latter exposure which gives MINOS/MINOS+ some sensitivity for detecting $\nu_\mu \to \nu_e$ appearance oscillations in the vicinity of the terrestrial MSW resonance.

Using its large exposure the medium-energy NuMI beam, MINOS+ is capable of identifying ν_e-CC interactions in the region $6 < E_\nu < 12\,\mathrm{GeV}$ with an efficiency of 78%. The experiment is using this capability to search for evidence of $\nu_\mu \to \nu_e$ that may be driven by coupling to sterile neutrino(s). Initial results from analysis of 2.97×10^{20} POT were reported at Neutrino 2016 [34] and at ICHEP 2016 [35]. For neutrino interactions in the 6-12 GeV range, the predicted number of candidate events CC-ν_e events assuming standard 3-flavor oscillations is 56.7 events. MINOS+ observes 78 events, an excess of $2.3\,\sigma$ [34].

The situation is somewhat different with respect to the OPERA experiment, originally designed to measure $\nu_\mu \to \nu_\tau$ oscillations. The experiment used the CERN CNGS ν_μ beam directed towards the OPERA emulsion "bricks" detector located 730 km away at the Gran Sasso Underground Laboratory. The beam is wide-band, with a flux that has a maximum 'flattop' extending from $\sim$ 8 GeV to 24 GeV, with $\langle E_\nu \rangle = 17$ GeV. The average detection efficiency for charged-current ν_e events is $\sim 15 \pm 3\%$ for $E_\nu < 10$ GeV, and $40 \pm 4\%$ for $10 < E_\nu < 20$ GeV [32]. The total exposure for the duration of the data-taking from 2008 to 2012 is 1.797×10^{20} POT. Preliminary results have been reported for the experiment's ν_e appearance search using the full data set [33].

Taking inspiration from these preliminary results, we have assembled predictions for the outcome of measurements from OPERA and MINOS+, where the latter would use the full MINOS+ exposure combined with the earlier MINOS ν_μ exposures. Our estimate builds upon distributions of charged-current (CC) event rate (e.g. the ν flux times CC-inclusive cross section vs. neutrino energy), which are available for the MINOS ν_μ exposure [36], for the MINOS+ exposure [37], and for OPERA exposure [32]. Estimates of detection rates for ν_e signal and background processes have been extracted from predictions given by MINOS+ [35], scaled to the appropriate POT exposure, and OPERA [33]. For MINOS+, the selection efficiency is assumed to be constant versus neutrino energy for all types of interaction, while for OPERA efficiencies are estimated for each bin of 10 GeV width and a linear interpolation is taken between bin centers. Neutral-current (NC) predictions are not affected by oscillations and are thus kept unchanged apart from the appropriate scaling with exposure.

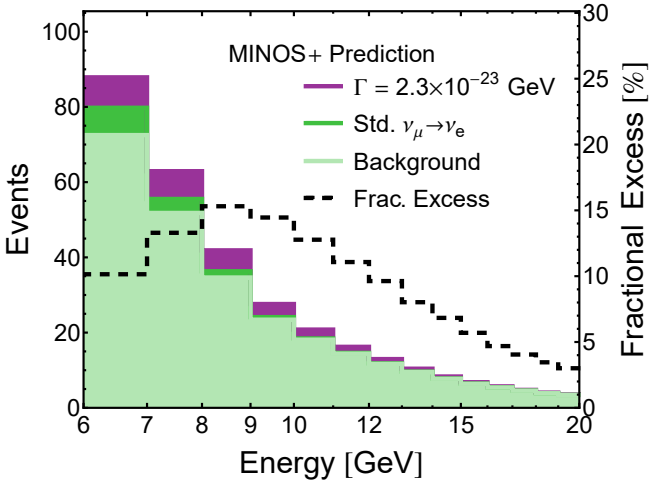

FIG. 2. Prediction for the excess of ν_e appearance events (uppermost histogram) that may occur in MINOS & MINOS+ data for the case of normal mass hierarchy. The enhanced ν_e rate arises from decoherence modification of the MSW resonance at $E_\nu = 12$ GeV. The estimation is based upon publicly presented fluxes and detection efficiencies and assumes investigation of the full $(10.56 + 10) \times 10^{20}$ POT exposures of MINOS and MINOS+ to the low-energy and medium-energy NuMI beams.

Based on these estimates, our prediction for a MINOS & MINOS+ analysis of a 6 GeV to 20 GeV search region in neutrino energy is presented in Fig. 2. The figure shows the predicted distribution of candidate ν_e events assuming that the decoherence-matter effect enhancement is operative and that the neutrino mass hierarchy is the normal hierarchy. The prediction indicates an excess of CC-ν_e candidates of $\sim$ 32 events above an expectation of 282 events based on conventional 3-flavor oscillations. If a binned analysis is performed, the full MINOS & MINOS+ data sample should be sensitive to this decoherence effect at $\sim 2\,\sigma$ statistical significance.

In OPERA, the number of candidate CC-ν_e events with $0 < E_\nu < 20$ GeV predicted for the case of SM 3-flavor ν oscillations (including backgrounds and 3-flavor ν_e signal), is 7.0 events; a total of 7 candidate events is observed. However in the presence of the decoherence-matter effect enhancement, the rate of genuine ν_e appearance events would receive a boost: Instead of OPERA's estimate of 1.4 ν_e-flavor events based upon conventional 3-flavor oscillations, the expected rate becomes $\sim$ 10.4 events. The candidate sample to be expected is then 16.0 events, to be compared to 7 observed events. Thus OPERA provides a test for the presence of the decoherence-matter effect enhancement in the case of normal hierarchy of $\sim 2.5\,\sigma$ statistical significance.

V. CONCLUSIONS

It is well-known that the terrestrial MSW matter effect, if subjected to experimental examination by mantle-crossing long-baseline $\nu_\mu/\bar{\nu}_\mu$ beams, can enable the hierarchy for neutrino mass states to be determined. This paper highlights the related but new phenomenon identified by R.L.N. Oliveira: environmental decoherence of oscillating neutrino states could make the MSW $\nu_\mu \to \nu_e$ resonance and hierarchy discrimination accessible to existing experiments whose baselines are confined to the Earth's crust [16]. We have identified OPERA and MINOS+ as two such experiments; both have reported preliminary measurements that have sensitivity to this phenomenon. Results reported thus far however are tantalizingly ambiguous. At the level of $\sim 2.5\,\sigma$ significance, OPERA observes no evidence for anomalous ν_e appearance for energies in the vicinity of the MSW resonance at 12 GeV. Their result indicates that, if the mass hierarchy is normal then decoherence is absent or is, at best, associated with a smaller Γ coupling than proposed by Ref. [6]. An opposite trend however – an excess of ν_e charged-current event candidates in the interval $6\,\mathrm{GeV} < E_\nu < 12\,\mathrm{GeV}$ – is observed in MINOS+ data. If the latter trend continues to hold in analysis of the experiment's full dataset, then decoherence with normal mass hierarchy offers a viable interpretation. This interpretation differs from the one that originally motivated the OPERA and MINOS+ investigations, namely that anomalous ν_e appearance may be the harbinger of coupling(s) to sterile neutrino(s). To the extent that the current situation becomes more widely appreciated and further experimental investigation is encouraged – this paper will have achieved its goal.

ACKNOWLEDGMENTS

This work was supported by the United States Department of Energy under grant DE-SC0007866 and by the IdEx program at Sorbonne Paris Cité (ANR-11-IDEX-0005-02).

[1] B. Pontecorvo, Sov. Phys. JETP **7**, 172 (1958); V. N. Gribov and B. Pontecorvo, Neutrino astronomy and lepton charge, Phys. Lett. B **28**, 493 (1969); Z. Maki, M. Nakagawa, and S. Sakata, Remarks on the unified model of elementary particles, Prog. Theor. Phys. **28**, 870 (1962).

[2] P. Adamson *et al.* (NOvA Collaboration), Measurement of the neutrino mixing angle θ_{23} in NOvA, Phys. Rev. Lett. **118**, 151802 (2017).

[3] I. Esteban, M. C. Gonzalez-Garcia, M. Maltoni, I. Martinez-Soler, and T. Schwetz, Updated fit to three neutrino mixing: exploring the accelerator-reactor complementarity, J. High Energy Phys. 087 (2017) 1.

[4] K. Abe *al.* (T2K Collaboration), Combined analysis of neutrino and antineutrino oscillations in T2K, Phys. Rev. Lett. **118**, 151801 (2017).

[5] Z. Xing and Z. Zhao, A review of $\mu - \tau$ flavor symmetry in neutrino physics, Rept. Prog. Phys. **79**, 076201 (2016).

[6] João A. B. Coelho, W. Anthony Mann, and Saqib S. Bashar, Nonmaximal θ_{23} mixing at NOvA from neutrino decoherence, Phys. Rev. Lett. 118, 221801 (2017).

[7] E. Lisi, A. Marrone, and D. Montanino, Probing possible decoherence effects in atmospheric neutrino oscillations, Phys. Rev. Lett. **85**, 1166 (2000).

[8] G.L. Fogli, E. Lisi, A. Marrone, D. Montanino, and A. Palazzo, Phys. Rev. D **76**, 033006 (2007).

[9] R. L. N. Oliveira, M. M. Guzzo, and P. C. de Holanda, Phys. Rev. D **89**, 053002 (2014).

[10] S. Weinberg, *Lectures on Quantum Mechanics* (Cambridge University Press, 2nd Edition, Cambridge, U.K. 2015), Sec. 6.9.

[11] J. Ellis, N. E. Mavromatos, and D. V. Nanopoulos, A microscopic Liouville arrow of time, Chaos, Solitons, and Fractals **10**, 345 (1999).

[12] G. Barenboim, N. E. Mavromatos, S. Sarker, and A. Waldon-Lauda, Quantum decoherence and neutrino data, Nucl. Phys. **B758**, 90 (2006).

[13] Y-L. Chan, M.-C. Chu, K. M. Tsui, C. F. Wong, J. Xu, Wave-packet treatment of reactor neutrino oscillation experiments and its implications on determining the neutrino mass hierarchy, Eur. Phys. J. C **76**, 310 (2016).

[14] F. P. An *et al.* (Daya Bay Collaboration), Study of wave packet treatment of neutrino oscillation at Daya Bay, arXiv:1608.01661.

[15] L. Wolfenstein, Neutrino oscillations in matter, Phys. Rev. D **17**, 2369 (1978); S. P. Mikheyev and A. Y. Smirnov, Resonant amplification of ν oscillations in matter and solar-neutrino spectroscopy, Yad. fiz. **42**, 1441 (1985) [Sov. J. Nucl. Phys. **42**, 913 (1985)]; S. P. Mikheyev and A. Y. Smirnov, Nuovo Cim. C **9**, 17 (1986).

[16] R. L. N. Oliveira, Dissipative effect in long-baseline neutrino experiments, Eur. Phys. J. C **76**, 417 (2016).

[17] J. Strait, LBNF neutrino beams, *in* Proc. 17th Int. Workshop on Neutrino Factories and Future Neutrino Facilities (NuFact15), eds. H. da Motta and J. Morfin, Rio de Janeiro, Brazil, 358 (2015).

[18] A. M. Gago, E. M. Santos, W. J. C. Teves, and R. Zukanovich Funchai, A study on quantum decoherence phenomena with three generations of neutrinos, [arXiv:hep-ph/0208166].

[19] R. L. N. Oliveira and M. M. Guzzo, Quantum dissipation in vacuum neutrino oscillation, Eur. Phys. J. C **69**, 493 (2010).

[20] R. L. N. Oliveira and M. M. Guzzo, Dissipation and θ_{13} in neutrino oscillations, Eur. Phys. J. C **73**, 2434 (2013).

[21] M. M. Guzzo, P.C de Holanda, and R. L. N. Oliveira, Quantum dissipation in a neutrino system propagating in vacuum and in matter, Nucl. Phys. **B908**, 408 (2016).

[22] G. Balieiro Gomez, M. M. Guzzo, P. C. de Holanda, and R. L. N. Oliveira, Parameter limits for neutrino oscillations with decoherence in KamLAND, Phys. Rev. D **95**,

113005 (2017).
[23] V. Gorini, A. Frigerio, M. Verri, A. Kossakowski, and E.C.G. Sudarshan, Properties of quantum Markovian master equations, Rep. Math. Phys. **13**, 149 (1978).
[24] G. Lindblad, On the generators of quantum dynamical semigroups, Commun. Math. Phys. **48**, 119 (1976).
[25] F. Benatti and R. Floreanini, Completely positive dynamical maps and the neutral kaon system, Nucl. Phys. **B488**, 335 (1997).
[26] Y. Farzan, T. Schwetz, and A. Y. Smirnov, Reconciling results of LSND, MiniBooNE and other experiments with soft decoherence, J. High Energy Phys. 807 (2008) 067; P. Bakhti, Y. Farzan, and T. Schwetz, Revisiting the quantum decoherence scenario as an explanation for the LSND anomaly, J. High Energy Phys. 2015 (2015) 007.
[27] M. Freund, Analytic approximations for three neutrino oscillation parameters and probabilities in matter, Phys. Rev. D **64**, 053003 (2001).
[28] F. Benatti and R. Floreanini, Massless neutrino oscillations, Phys. Rev. D **64**, 085015 (2001).
[29] A. Cervera, A. Donini, M.B. Gavela, J.J. Gomez Cádenas, P. Hernández, O. Mena, and S. Rigolin, Golden measurements at a neutrino factory, Nucl. Phys. **B579**, 17 (2000), Erratum-ibid, **B593**, 731 (2001).
[30] P. Lipari, Matter effects in long-baseline experiments, the flavor content of the heaviest (or lightest) neutrino and the sign of Δm^2, Phys. Rev. D **61**, 113004 (2000).
[31] I. Esteban *et al.*, Updated fit to three neutrino mixing: exploring the accelerator-reactor complementarity, J. High Energy Phys. 01 (2017) 087; arXiv:1611.01514.
[32] N. Agafonova *et al.* (OPERA Collaboration), Search for $\nu_\mu \to \nu_e$ oscillations with the OPERA experiment in the CNGS beam, J. High Energy Phys. 07 (2013) 004; arXiv:1303.3953.
[33] G. De Lellis, for the OPERA Collaboration, Results of the OPERA experiment, Talk at the CXXVI SPSC Meeting, June 2017: https://indico.cern.ch/event/645753/?view=nicecompact;
S. Vasina, for the OPERA Collaboration, Results from the OPERA experiment, to appear in Proceedings; talk at the Rencontres du Vietnam, Quy Nhon, July 2017. http://vietnam.in2p3.fr/2017/neutrinos/program.php.
[34] J. Evans, for the MINOS+ Collaboration, New results from the MINOS+ experiment, to appear in Proceedings; see slides 21,22 of Talk at *Neutrino 2016*, London, United Kingdom, July 2016.
[35] L. Whitehead, Sterile Neutrino Searches with MINOS/MINOS+, talk at ICHEP, Chicago, August 2016. https://indico.cern.ch/event/432527/contributions/2181989/.
[36] Z. Pavlovic, Observation of Disappearance of Muon Neutrinos in the NuMI Beam, Ph.D. thesis, University of Texas, 2008 [Report No. FERMILAB-THESIS-2008-59].
[37] J. Todd, Search for sterile neutrino oscillations in muon neutrino disappearance at MINOS/MINOS+, talk at the APS April Meeting 2017. https://meetings.aps.org/Meeting/APR17/Session/J11.8.